GEOMETRIC CAPITULUM PATTERNS BASED ON FIBONACCI p-PROPORTIONS

BRUCE M. BOMAN

Abstract. Modeling based on the golden angle has provided valuable insight into how densely packed phyllotaxis structures and organizational patterns arise. The classic example is the phyllotactic model based on the golden angle for organization of florets on a sunflower. Previous studies of geometric pattern generation show that structure organization and covering is highly sensitive to the angle of intersection of pairs of phyllotactic spirals (parastichies). In biology, these patterns arise in a meristem of the primordium and the golden angle of parastichy pairs produces an optimal packing density. Consequently, packing efficiencies and organization of coverings of a geometric capitulum can be modeled and its properties analyzed according to angle of rotation which produces a spiral pattern. To begin to understand how other phyllotaxis patterns might arise, different geometric patterns were generated based on the generalized golden p-sections, which are linked to the Fibonacci p-numbers. Generation of various geometric structures shows that different efficiencies of covering and regular organizational patterns occur across different golden p-proportions. Conclusion: studying geometric capitulum patterns based on golden p-ratios begins to show how geometric tissue patterns might occur in biology.

Contents

1. INTRODUCTION

Multicellular life evolved on earth about 600 million years ago [1], but how multicellular organisms develop and maintain organization of their tissues is still a mystery. Pattern recognition in phyllotaxis research coupled with mathematical modeling has provided important insight into mechanisms that help explain tissue organization [2, 3]. Geometric patterns observed in histologic structures of plants and animals are often described by the Fibonacci numbers. Indeed, Fibonacci numbers often appear in number of flower petals, spirals on a sunflower or nautilus shell, starfish, and fractions that appear in phyllotaxis [4, 5, 6, 7]. While

the regularity of these patterns in biology can be described by the Fibonacci numbers, the processes that generate these structures are still being elucidated. This raises the question: What biologic rules and mathematical laws that control the growth and renewal of tissues in multi-cellular organisms give rise to these patterns of Fibonacci numbers? To begin to understand how these patterns arise, we have been studying different patterns that might arise based on Fibonacci p-numbers [8, 9].

In one study, we created a cell division model for tissue organization based on the biology of tissue renewal [10]. This model builds upon the cell maturation concept posed in the Spears and Bicknell-Johnson model for asymmetric cell division [11, 12]. Based on the process of asymmetric cell division, model output simulated the dynamic growth of cell populations and generation of hierarchical patterns found in tissues. Importantly, our model [10] generated complex dynamic patterns in which organization of cells in tissues remained constant despite continuous cell division occurring within the tissue structure. Thus, by modeling the spatial and temporal asymmetries of cell division, we discovered that simple rules can explain how tissue organization is maintained during tissue renewal in biology. In another study [13], we studied geometric branching patterns based on Fibonacci p-sequences that revealed how the regularity in branching patterns might occur in biology. This modeling also showed generation of branching structures produces patterns of self-similarities that occur across different degrees of branching and multiple dimensions. Our studies demonstrated that geometric characterization of Fibonacci p-numbers can help us understand the biological rules that underlie branching patterns in nature.

The current study builds upon the Fibonacci p-number series by investigating geometric capitulum patterns that are formed based on golden p-proportions. Many important studies on the golden angle have provided an understanding of how densely packed phyllotaxis structures and organizational patterns arise in biology [2, 3, 4, 5, 6]. The classic example being the geometric pattern produced by the golden angle that simulates the organization of florets on a sunflower. Other studies of geometric pattern generation [14] revealed that structure organization and coverings are highly sensitive to the angle separating individual primordia. Such organization arises in a meristem with the Fibonacci angle producing parastichy having an optimal packing density [15]. In other studies of phyllotaxis [2, 3, 16, 17], packing efficiencies and organization of a covering of a geometric capitulum are modeled according to different angles of rotation which produces various circular patterns. Angles that are only a rational fraction of a turn generally produce very poor coverings while the golden angle produces one of the best coverings. Accordingly, to further understand how other phyllotaxis patterns might arise, different geometric patterns were generated herein based on the generalized golden p-sections, which are linked to the Fibonacci p-numbers [8, 9].

2. PREVIOUS RESULTS

In our recent study [13], we investigated the generalized golden p-sections (Figure 1) that are associated with patterns of asymmetric cell division in tissues. We discovered that the generalized golden p-sections can be modeled as branching structures based on a specific number of decreasing-sized branches that arise from a main branch. It was assumed that the ratio between the sizes of pairs of consecutive branches (ordered by size) equals the ratio of the largest branch size to the next branch size and all other branches follow this same ratio (Figure 2). We observed that the original expressions for the generalized golden p-sections were still retained by the expressions in our new branched geometric structures (Figure 3). Our modeling using these new expressions produced different branching patterns that emerged over time. These

geometric structures also allowed us to create corresponding agent-based models to further study different branching patterns and analyze the dynamics of these patterns as they emerge over time [13]. The study herein builds on this geometric property to identify patterns formed in geometric capitulum structures.

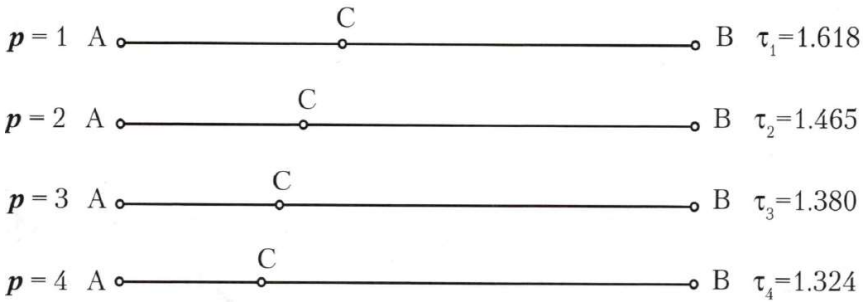

FIGURE 1. Geometric expression of the Fibonacci p-numbers [9]. The golden p-ratio is the ratio of two quantities CB and AC if their ratio is the same as the ratio of two larger quantities AB and CB raised to the power p. Algebraically, for AB, CB, and AC with $AB > CB > AC$, the ratio is $\varphi_p = \frac{CB}{AC} = (\frac{AB}{CB})^p$, where the Greek letters(φ_p, τ_p or Φ_p) represent the golden p-ratio [8-13]. It is also the positive root that is a solution to the quadratic equation $\varphi_p^{p+1} - \varphi_p^p = 1$.

The Fibonacci p-numbers, denoted F_p, are a generalization of the well-known Fibonacci numbers. Fibonacci p-numbers form a sequence, the Fibonacci p-sequence (Table 1), whereby each number is the sum of two preceding ones based on the recursive relation for $n > p + 1$: $F_p(n) = F_p(n-1)+F_p(n-p-1)$, and $F_p(0) = 0$, $F_p(1) = F_p(2) = \ldots = F_p(p) = F_p(p+1) = 1$.

Fibonacci p-numbers are closely linked to the golden p-ratio. For $p = 1$ that represents the Fibonacci sequence, the Fibonacci numbers are related to the classic golden ratio. The Binet formula gives the n^{th} Fibonacci number in terms of n and the golden ratio [9]. It designates that as n increases, the ratio of two consecutive Fibonacci numbers tends to the golden ratio.

$$F_n = \frac{\varphi^n - \psi^n}{\varphi - \psi} = \frac{\varphi^n - \psi^n}{\sqrt{5}}, \text{ where } \varphi = \frac{1+\sqrt{5}}{2} \approx 1.618034 \text{ and } \psi = \frac{1-\sqrt{5}}{2} \approx 0.618034.$$

A generalized Binet formula for Fibonacci p-numbers is derived by Kilic and Stakhov [8, 9].

TABLE 1. The Fibonacci p-number sequence ($p = 2$ to 5)

***p*-value**	**OEIS number**	**Fibonacci *p*-number sequence**
$p = 2$	A000045	1, 1, 1, 2, 3, 4, 6, 9, 13, 19, 28, 41, 60, 88, 121, 181, ...
$p = 3$	A000930	1, 1, 1, 1, 2, 3, 4, 5, 7, 10, 14, 19, 26, 36, 50, 69, 95, ...
$p = 4$	A003269	1, 1, 1, 1, 1, 2, 3, 4, 5, 6, 8, 11, 15, 20, 26, 34, 45, 60, ...
$p = 5$	A003520	1, 1, 1, 1, 1, 1, 2, 3, 4, 5, 6, 7, 9, 12, 16, 21, 27, 34, 43, ...
Online Encyclopedia of Integer Sequences (OEIS) numbers from `https://oeis.org/`		

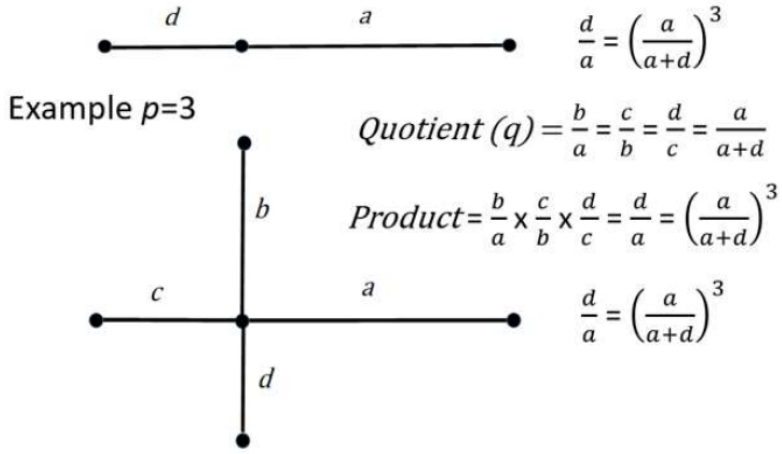

FIGURE 2. A geometric branching pattern was created for $p = 3$ based on a specific number of decreasing-sized branches that arise from a main branch [13]. The quotient(q-ratio) between the sizes of pairs of consecutive branches (ordered by size) equals the ratio of the largest branch size to the sum of the largest and smallest branch sizes. The q-ratio is also the reciprocal of the golden p-ratio.

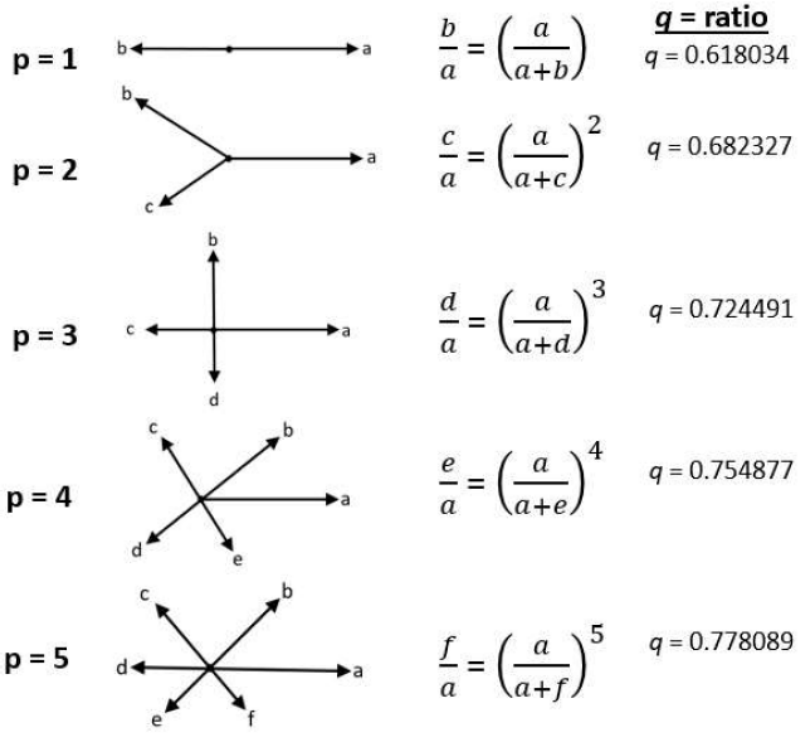

FIGURE 3. Geometric branching pattern based on the generalized golden p-sections for $p = 1$ to 5. The q-ratio is given for each p-value. For $p = 1$, the structure is known as the golden section.

3. NEW RESULTS

3.1. **Supergolden Rectangles.** To explore whether other possible geometric patterns exist based on these geometric branching patterns, it was determined if supergolden rectangles might be created based on the golden p-proportions. The classic golden rectangle is linked to the golden ratio ($\varphi = 1.618034$), which has been extensively studied [4, 6, 9, 18, 19]. The supergolden rectangle (Figure 4) is constructed by creating a geometric structure that subdivides a rectangle so that $ABCD$, $EHGD$, and $HFCG$ are similar [19, 20].

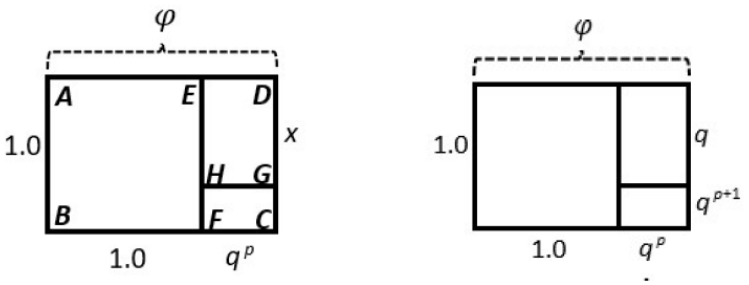

FIGURE 4. The supergolden rectangle was created based on the geometric q-ratios.

The length of the supergolden rectangle (AD and BC) equals the value of generalized golden p-section (φ). As $\varphi^{p+1} = \varphi^p + 1$ (mentioned earlier in Figure 1), using $\varphi = \frac{1}{q}$, we get on dividing by φ^p, the equation $\varphi = 1 + \frac{1}{\varphi^p}$, so $\varphi = 1 + q^p$, or $\frac{1}{q} = 1 + q^p$, which gives $1 = q + q^{p+1}$. It is then simple to solve for x because $ABCD$ and $EHGD$ are similar, so x equals q and $1 - x = q^{p+1}$. The supergolden rectangle for $p = 2$ has previously been reported [19, 20, 21]. The supergolden rectangles for $p = 3$ to 5 as well as the structure for any generalized golden p-section were created herein and are illustrated in Figures 4 and 5.

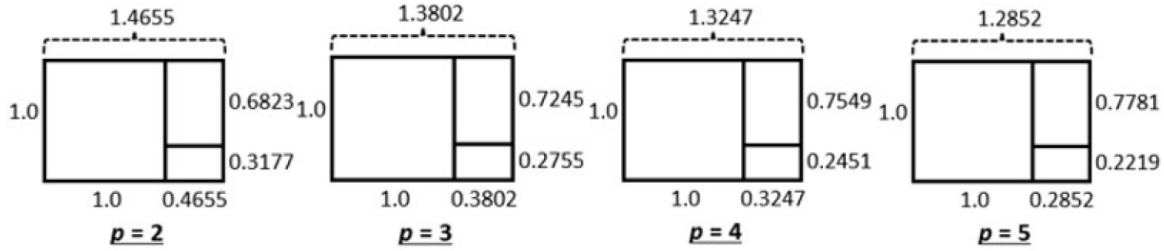

FIGURE 5. The supergolden rectangles for generalized golden p-sections $p = 2$ to 5.

3.2. **Geometric Capitulum Patterns on a Disk.** To identify other structures that might be established based on expression of the p-Fibonacci numbers, the centric model for geometrical representation of plant and animal structures was explored. Indeed, this model has formed the cornerstone of research in phyllotaxis. For example, the geometric structures that are generated based on divergence angles for number sequences in Table 2 [3] produce patterns that have parastichy pairs observed in plants of the *Asteraceae* flowering plant species [22, 23]. This biologic family has over 25,000 species! The geometric capitulum patterns that are generated on a disk by the known divergence angles (Table 2) were plotted herein and are shown in Figure 6 below.

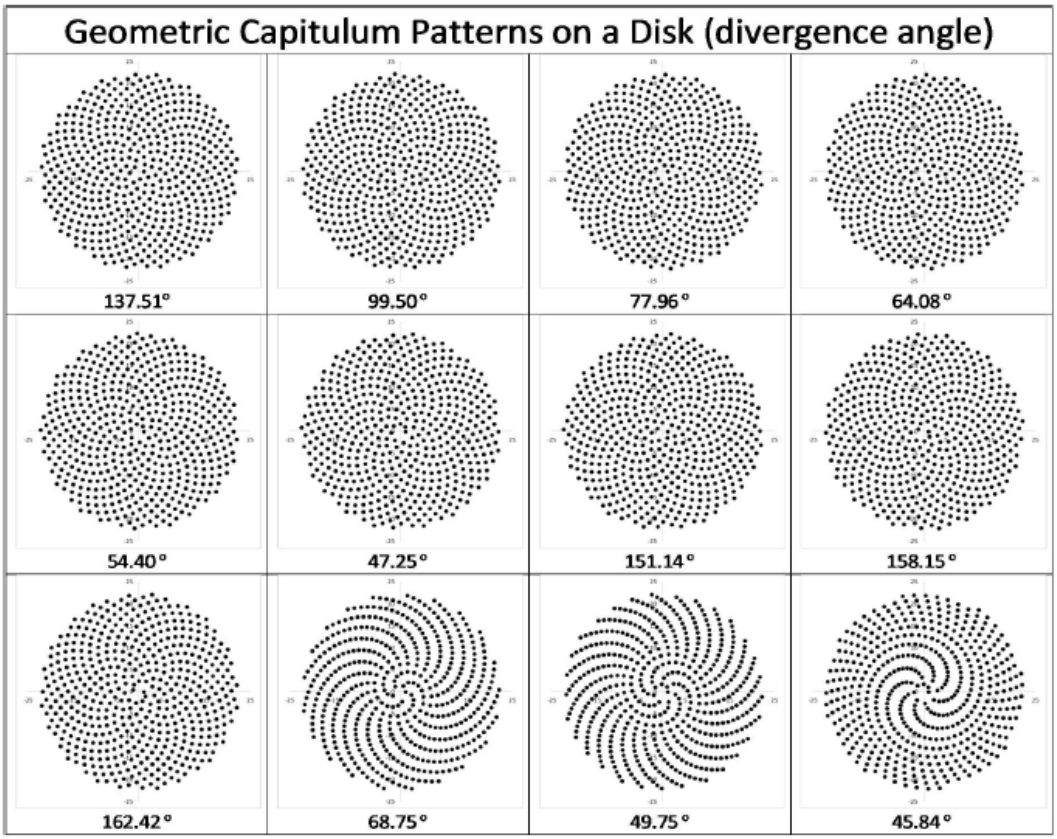

FIGURE 6. Geometric capitulum patterns on a disk plotted based on the divergence angle. Patterns were generated using 2D polar coordinates according to the method outlined in reference [24].

3.3. **Sectioning the Circle Circumference based on Fibonacci p-Proportions.** The centric model for generating geometrical patterns was then pursued to study other possible manifestations of the p-Fibonacci numbers. Accordingly, the circle circumference was sectioned into fractions based on the generalized golden p-sections (Figure 7). The arc lengths (a, b, c, d, e, and f) correspond to branch sizes and properties illustrated in Figure 3. The ratio of the length of the smallest arc to that of the largest arc equals the ratio of the large arc to the circle circumference. The length of adjacent arcs (small/large) equals the q-ratio corresponding to each golden p-proportion (Figure 3). So, the fraction of the circumference (f) subtended by each of the arcs can be determined as well as the respective central angles of the circle. For $p = 1$, the fraction of the circumference of the small arc (0.3819) corresponds to the golden angle [25].

3.4. **Geometric Capitulum Patterns based on Fraction of Circumference.** Geometric capitulum patterns were then generated on a disk using the fraction of the circumference corresponding to each of the generalized golden p-sections. The approach relied on the polynomials for the generalized golden p-sections that describe ratios of branch sizes (i.e. q-ratios) in Figure 3 as given in Table 3. Then, polynomial expressions corresponding to each p-value were expanded (Table 3, Appendix A) and the q-values in the expanded polynomials were

TABLE 2. Divergence angles for number sequences ($p = 1$) that correspond to geometric patterns of phyllotaxis [3]. Divergence angle is defined as "the two angles at the center of a transverse section of a growing root tip determined by consecutively initiated primordia" [3]. Fraction of the circumference is calculated by dividing the divergence angle by 360^o.

Divergence Angle	Fraction of Circumference	Number Sequence
137.51°	0.381972	1, 2, 3, 5, 8, 13, 21, 34, 55, ...
99.50°	0.276389	1, 3, 4, 7, 11, 18, 29, 47, 76, ...
77.96°	0.216556	1, 4, 5, 9, 14, 23, 37, 60, 97, ...
64.08°	0.178	1, 5, 6, 11, 17, 28, 45, 73, 118, ...
54.40°	0.151111	1, 6, 7, 13, 20, 33, 53, 86, 139, ...
47.25°	0.13125	1, 7, 8, 15, 23, 38, 61, 99, 160, ...
151.14°	0.419833	2, 5, 7, 12, 19, 31, 50, 81, 131, ...
158.15°	0.439306	2, 7, 9, 16, 25, 41, 66, 107, 173, ...
162.42°	0.451167	2, 9, 11, 20, 31, 51, 82, 133, 215, ...
68.75°	0.190972	2 (1, 2, 3, 5, 8, 13, 21, 34, 55, ...)
49.75°	0.138194	2 (1, 3, 4, 7, 11, 18, 29, 47, 76, ...)
45.84°	0.127333	3 (1, 2, 3, 5, 8, 13, 21, 34, 55, ...)

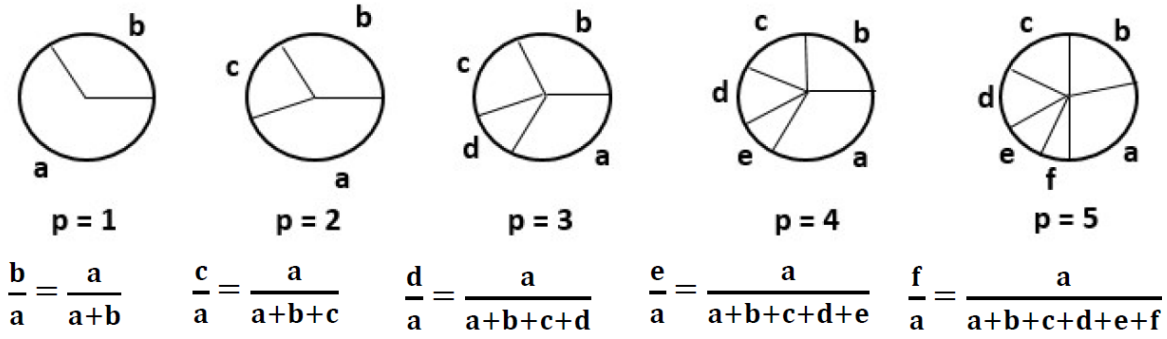

FIGURE 7. Division of the circle circumference into fractions based on the *q*-ratios. The arc lengths (a, b, c, d, e, f) correspond branch sizes in Figure 3.

correlated with the fractions of the circumference in Figure 8. The angle that is subtended by each fraction of the circumference was then used to create a geometric capitulum pattern.

The resulting geometric disk patterns (Figure 9) showed that all of them have a spiral configuration and very uniform coverings. None of these patterns exhibit obvious parastichy pairs that correspond to the *p*-number sequences. The disk patterns for q and q^{p+1} for each *p*-proportion ($p = 1$ to 5) were identical because of the relationship $q + q^{p+1} = 1$. Several disk patterns, $p = 2(q^4)$, $p = 3(q^4)$, $p = 4(q^6)$, and $p = 5(q^7)$, show highly dense coverings. But these disk patterns having a high density have an arc length that is close to the value of an arc length (Table 2) corresponding to one of geometric patterns shown in Figure 6. However, overlay of the different patterns (Figure 9) corresponding to each *p*-value ($p = 2$ to 5) produced highly dense coverings and the cells in each covering did not appear to overlap.

TABLE 3. Polynomial expressions for Fibonacci p-number sequence ($p = 2$ to 5) based on q-ratio.

p-value	Polynomial Expression	Expanded Polynomial Expression
$p = 2$	$q^3 + q = 1$	$q^4 + q^3 + q^2 = 1$
$p = 3$	$q^4 + q = 1$	$q^6 + q^5 + q^4 + q^3 = 1$
$p = 4$	$q^5 + q = 1$	$q^8 + q^7 + q^6 + q^5 + q^4 = 1$
$p = 5$	$q^6 + q = 1$	$q^{10} + q^9 + q^8 + q^7 + q^6 + q^5 = 1$

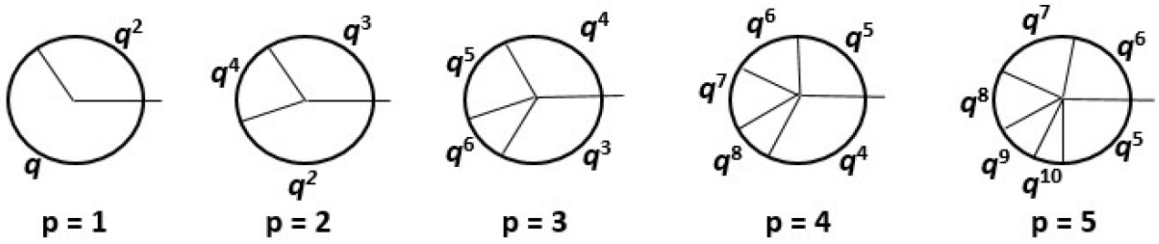

FIGURE 8. Circle circumference sections based on the expanded polynomial equations.

4. DISCUSSION AND CONCLUSIONS

All living multi-cellular organisms maintain themselves in a highly ordered state. Understanding the biologic rules that explain how organisms maintain proper organization of cells within their tissues is key to understanding of life itself. The organization of plant structures has been subject of much study in phyllotaxis. The structure of animal tissues is mainly pursued in histology and anatomy. Both fields show that tissue structure stays constant, making it appear static, when in fact tissues are continuously undergoing growth and renewal. Indeed, our previous modeling of asymmetric cell division [10, 13] helps us understand how the organization of cells in tissues remains constant despite continuous cell division occurring within the tissue structure.

Fibonacci numbers have given us great insight into tissue organization. The design of plants follows specific patterns that are frequently described by a Fibonacci sequence. Although not commonly recognized, animal tissues can also have a patterned structure that is described by the Fibonacci sequence. The classic example is invertebrate animals such as jellyfish. Since Fibonacci sequences appear so frequently in nature, it clearly indicates that this does not happen randomly or by accident. This gap in our knowledge has prompted me to study how patterned structures arise in biology. So the question becomes: what mechanisms explain Fibonacci number patterns in tissue biology?

This work focused on studying different geometric patterns that arise based on Fibonacci p-proportions. The basis for studying the Fibonacci p-numbers is that the p-number sequence is linked to cell population growth dynamics of proliferation that occurs in biology due to asymmetric cell division [10, 11, 13]. Indeed, asymmetric cell division is the cellular mechanism that is essential for proper tissue renewal and wound healing. The current study builds upon the Fibonacci p-number series by investigating geometric capitulum patterns that are formed based on the golden p-proportions. Investigation of geometric capitulum patterns helps us understand how the angle and rotation of cell division control tissue organization. The results

show that geometric structures are linked to the generalized golden p-sections including the supergolden rectangle and organization of a covering of a geometric disk. Specifically, these geometric structures can be described mathematically based on the q-ratio and the golden p-proportions. Our previous model also revealed that characteristics of branching can be described mathematically based on branch ratios (q) and the degree of branching (p).

The current results show that organized geometric disk patterns are generated for each of the generalized golden p-proportions. When geometric disk patterns are overlaid, there was little, or even no, overlap between the parastichies generated by the different angles of rotation. This result using modeling in 2D may begin to help understand how multi-cellular tissues are organized in 3D based on asymmetric cell division. Thus, modeling organized patterns based on the Fibonacci p-numbers can contribute to our understanding of how asymmetric cell division controls tissue structure in biology, particularly the organization of different cell types within tissues.

5. FURTHER WORK AND QUESTIONS

Since our modeling of the generalized golden p-proportions generates geometric patterns with self-similarity across multiple dimensions [13], it will be important to model the geometric patterns in 3D based on the Fibonacci p-proportions. Taking this approach, it may be possible to begin to geometrically characterize living histologic tissues using the p-Fibonacci sequences. An initial strategy might be to analyze geometric patterns generated by the Fibonacci p-proportions using the cylindrical lattice. This approach could build on the work by Spears et al. [12] on Fibonacci phyllotaxis involving models of asymmetric cell division using mapping of cylindrical patterns. Although understanding how geometric patterns normally appear in nature is an important question, another reason to discover the biologic rules that control normal tissue structure is to understand how tissue disorganization might occur in cancer and other diseases.

APPENDIX A. EXPANSION OF POLYNOMIAL EQUATIONS.

The expansion of the polynomial equations relating to the different p-values is obtained by the following simple approach.

If the general polynomial expression for Fibonacci p-number sequences based on q-ratios is $q^{p+1} + q = 1$, multiplying both sides of the equation by q gives $q^{p+2} + q^2 = q$.

Then substituting this expression for q back into the original equation gives an expanded expression. For example, $q^3 + q = 1$ can be expanded to $q^4 + q^3 + q^2 = 1$.

Using this same approach in a repetitive manner, it can expand the other polynomial expressions corresponding to Fibonacci p-number sequences $p = 3$ to 5 (Table 3), and to any expressions corresponding to larger p values.

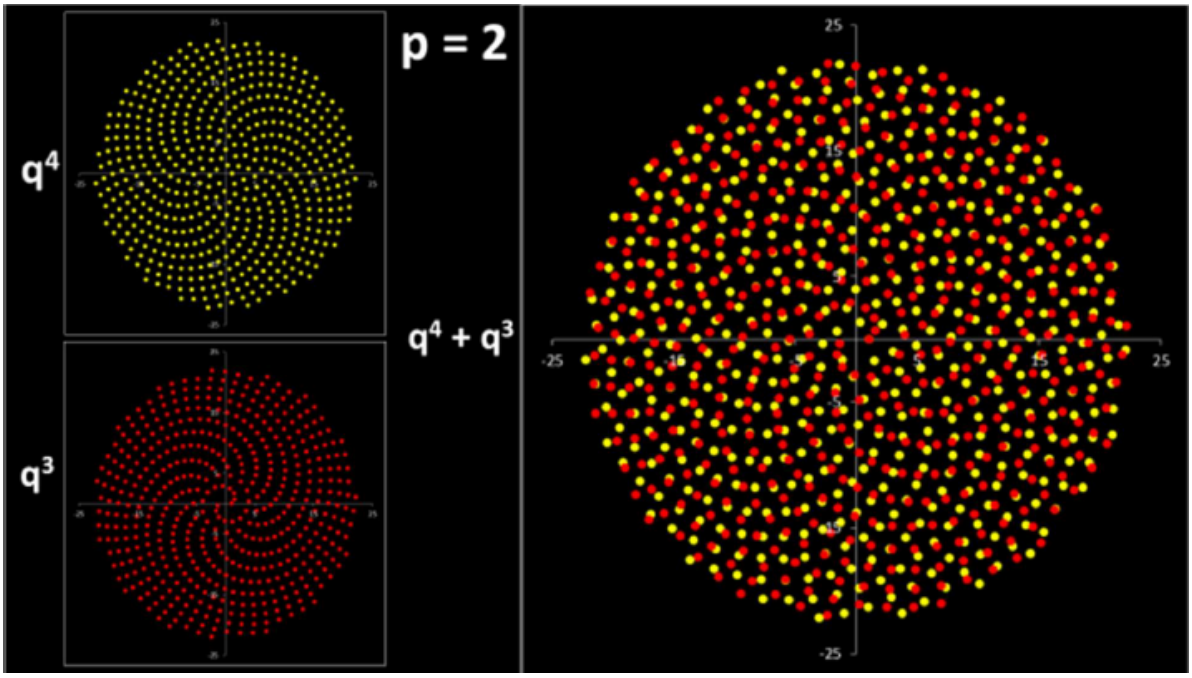
p = 2
q^4
q^3
$q^4 + q^3$

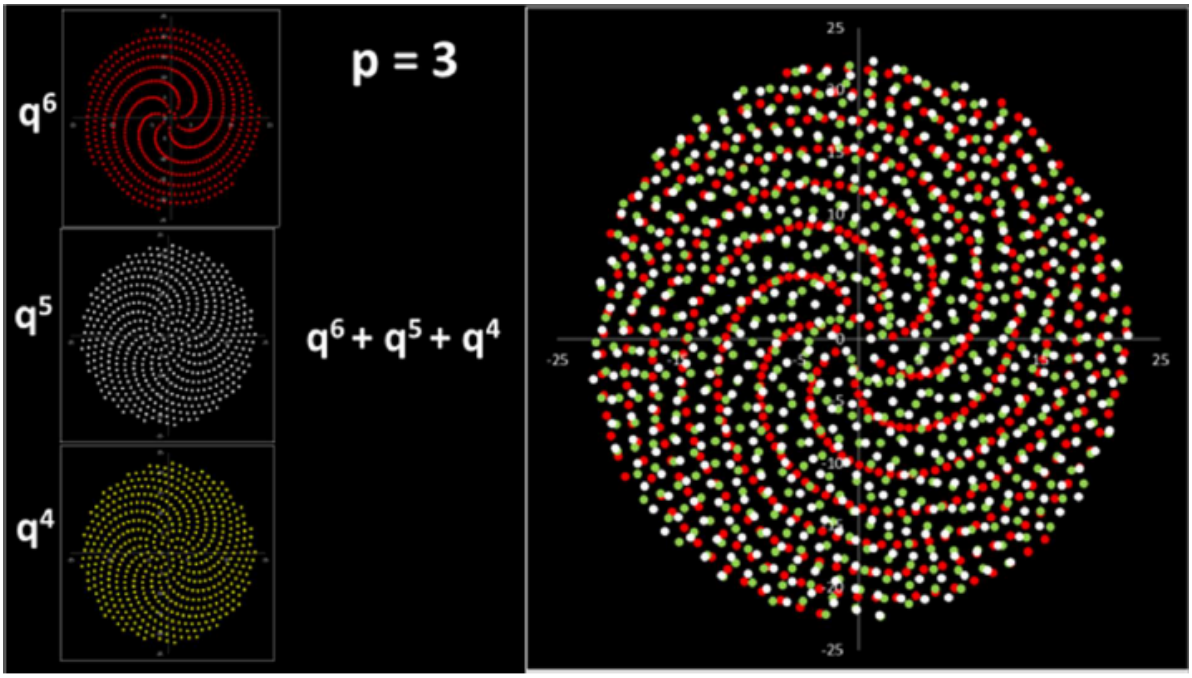
p = 3
q^6
q^5
q^4
$q^6 + q^5 + q^4$

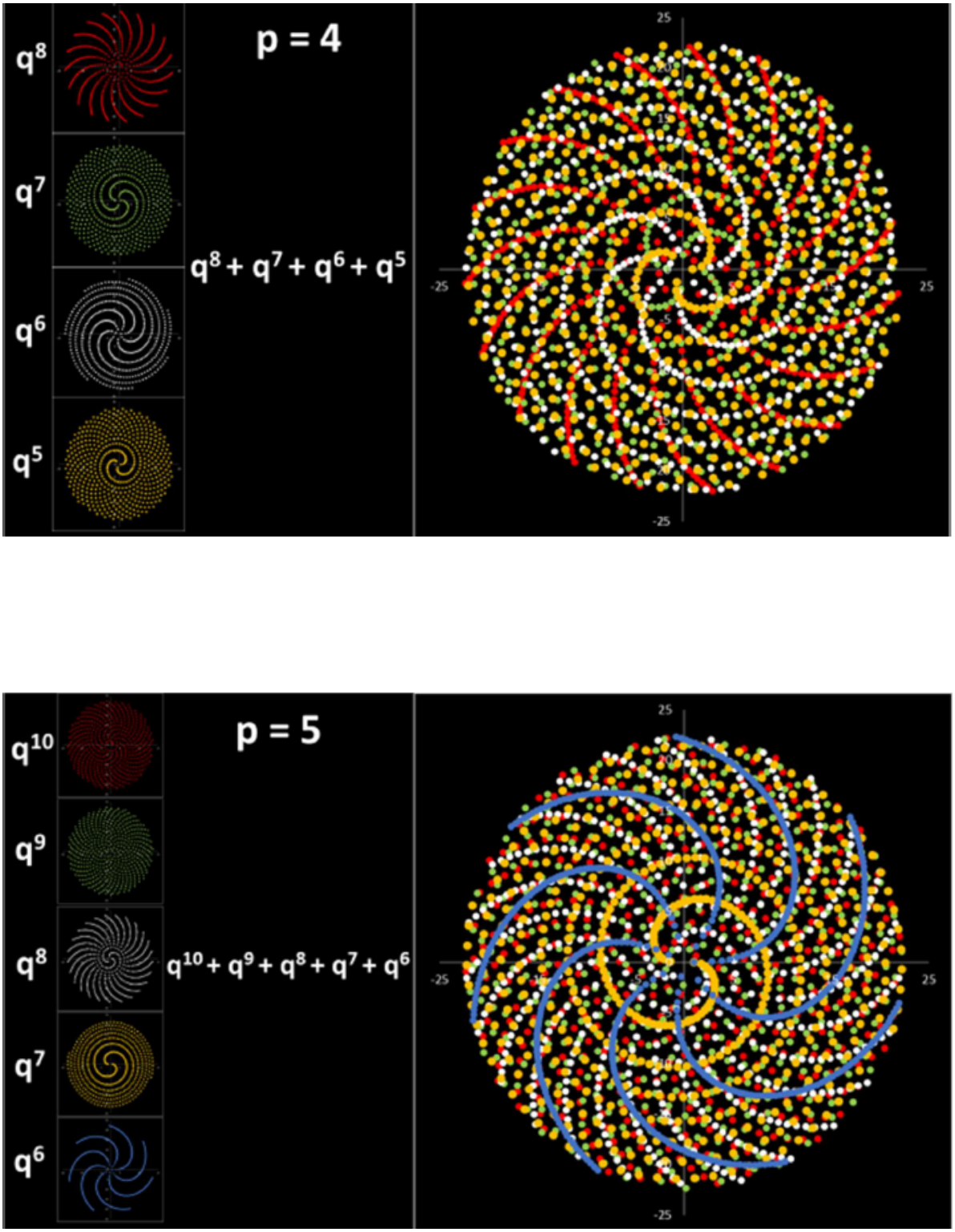

FIGURE 9. Geometric capitulum patterns generated by the different arc lengths (Figures 7 & 8).

References

[1] E. Libby and W. C. Ratcliff, Ratcheting the evolution of multicellularity, *Science* **346** (2014), no. 6208, 426–427.
[2] I. Adler, A model of contact pressure in phyllotaxis, *J. Theor. Biol.* **45** (1974), no. 1, 1–79.
[3] R. V. Jean, *Phyllotaxis: A Systemic Study in Plant Morphogenesis*, Cambridge University Press, 1994.
[4] M. Livio, *The Golden Ratio*, Broadway Books, New York, NY, 2002.
[5] I. Stewart, Florally finding Fibonacci. *The Mathematics of Life*, Basic Books, New York, 2011.
[6] R. Knott, *Fibonacci Numbers and Nature*, web resource avialable at http://www.maths.surrey.ac.uk/hosted-sites/R.Knott/Fibonacci/fibnat.html.
[7] M. H. Ross and W. Pawlina, *Histology: A Text and Atlas: With Correlated Cell and Molecular Biology, 7th Ed.*, Wolters Kluwer,, 2015.
[8] E. Kilic, The Binet formula, sums and representations of generalized Fibonacci p-numbers, *European J. Combin.* **29** (2008), no. 3, 701–711.
[9] A. Stakhov and S. Olsen, *The Mathematics of Harmony: From Euclid to Contemporary Mathematics and Computer Science*, World Scientific Publishing, Hackensack, NJ, 2009. pp. 186–254.
[10] B. M. Boman, T. Dinh, K. Decker, B. Emerick, C. Raymond, and G. Schleiniger, Why do Fibonacci numbers appear in patterns of growth in nature? A model for tissue renewal based on asymmetric cell division, *Fibonacci Quart.* **55** (2017), no. 5, 30–41.
[11] C. P. Spears and M. Bicknell-Johnson, Asymmetric cell division: binomial identities for age analysis of mortal vs. immortal trees, in *Applications of Fibonacci Numbers, Vol. 7*, edited by G. E. Bergum, A. N. Philippou and A. F. Horadam, Kluwer Academic Publishers, Dordrecht, 1998, pp. 377–391.
[12] C. P. Spears, M. Bicknell-Johnson, and J. J. Yan, Fibonacci phyllotaxis by asymmetric cell division: Zeckendorf and wythoff trees, *Congressus Numerantium* **201** (2010), 257–271.
[13] B. M. Boman, Y. Yihan, K. Decker, C. Raymond, and G. Schleiniger, Geometric branching patterns based on p-Fibonacci sequences: Self-similarity across different degrees of branching and multiple dimensions, *Fibonacci Quart* **57** (2019), no. 5, 29–41.
[14] C. Impens @ Valvas, Most rare: Mathematical proof of the golden angle. https://ci47.blogspot.com/2018/04/most-rare-mathematical-proof-of-golden.html.
[15] J. Ridley, Packing efficiency in sunflower heads, *Math. Biosci.* **58** (1982), no. 1, 129–139.
[16] S. Wundrak, J. Paul, J. Ulrici, E. Hell, and V. Rasche, A small surrogate for the golden angle in time-resolved radial MRI based on generalized Fibonacci sequences, *IEEE Trans. Med. Imaging* **34** (2014), no. 6, 1262–1269.
[17] R. Negishi, K. Sekiguchi, Y. Totsuka, and M. Uchida, Determining parastichy numbers using discrete Fourier transforms, *Forma* **32** (2017), 19–27.
[18] https://en.wikipedia.org/wiki/Goldenrectangle.
[19] A. J. Crilly, Golden rectangles, *50 Mathematical Ideas You Really Need to Know, 8th Edition, Quercus-Publishing, London*, 2007.
[20] T. Crilly, A supergolden rectangle, *Math. Gaz.* **78** (1994), no. 483, 320–325.
[21] https://en.wikipedia.org/wiki/Supergoldenratio.
[22] https://www.britannica.com/topic/list-of-plants-in-the-family-Asteraceae-2040400.
[23] https://en.wikipedia.org/wiki/Asteraceae.
[24] https://www.bing.com/videos/search?q=golden+angle%20+excell&&view=detail&mid=EF49A8C715193C280904EF49A8C715193C280904&&FORM=VRDGAR&ru=%20%2Fvideos%2Fsearch%3Fq%3Dgolden%2520angle%2520excell%26qs%3Dn%26form%3DQBVR%26sp3D-1%26pq%3Dgolden%2520angle%2520excell%26sc%3D0-19%26sk%3D%26cvid3D5D0FCB7C4E7F4D468C969C50B628D23F. Accessed 11/28/2020.
[25] https://en.wikipedia.org/wiki/Goldenangle.

Center for Applications of Mathematics in Medicine, Department of Mathematical Sciences, University of Delaware, Newark, DE 19716
E-mail address: brucemboman@gmail.com